Tectonophysics 507 (2011) 16–25

Contents lists available at ScienceDirect

Tectonophysics

journal homepage: www.elsevier.com/locate/tecto

Rapid locking of tectonic magnetic fabrics in weakly deformed mudrocks

Juan C. Larrasoaña [a,*], Miriam Gómez-Paccard [b], Santiago Giralt [b], Andrew P. Roberts [c]

[a] Instituto Geológico y Minero de España, Unidad de Zaragoza, Manuel Lasala 44 9B, Zaragoza 50006, Spain
[b] Institute of Earth Sciences Jaume Almera, CSIC, Lluís Solé i Sabarís s/n, Barcelona 08028, Spain
[c] Research School of Earth Sciences, The Australian National University, Canberra, ACT 0200, Australia

ARTICLE INFO

Article history:
Received 4 January 2011
Received in revised form 9 May 2011
Accepted 10 May 2011
Available online 18 May 2011

Keywords:
Magnetic fabric
Mudrocks
Active tectonics
Fold-and-thrust belt
Lake Issyk-Kul
Holocene

ABSTRACT

The anisotropy of magnetic susceptibility (AMS) has provided important insights into early deformation conditions in compressive settings through characterization of tectonic fabrics in mudrocks that appear otherwise undeformed. The validity of these insights relies on the assumption that tectonic fabrics are rapidly locked shortly after sediment deposition. However, the time lag between deposition and the tectonic overprint has yet to be quantified to verify this assumption. Here we present AMS data from Late Holocene sediments recovered in two cores from Lake Issyk-Kul in the Kyrgyz Tien Shan fold-and-thrust belt. These sediments, in which magnetic fabrics reflect the preferred orientation of phyllosillicates, have typical tectonic magnetic fabrics with varying degrees of tectonic overprint likely controlled by small-scale active faults. The mean orientation of the susceptibility maxima parallels neighbouring active thrust faults and is perpendicular to the geodetically-derived local shortening direction. The age model for one of the studied cores, which is based on 7 calibrated accelerator mass spectrometer radiocarbon dates, indicates that sediments as young as 25 yr record this clear tectonic fabric, which is locked within sediments older than 1180 cal. yr BP. Our demonstration of rapid locking of tectonic fabrics in weakly deformed mudrocks shortly after deposition provides the required validation of their reliability for tectonic studies, and opens new opportunities for providing quantitative insights into the relationship between magnetic ellipsoids, shortening rates, and stress directions in compressive settings.

1. Introduction

Magnetic fabrics have provided insights into early deformation conditions in fold-and-thrust belts (Aubourg et al., 1995; Borradaile and Henry, 1997; Borradaile and Jackson, 2004, 2010; Borradaile and Tarling, 1981; Cifelli et al., 2009; Kissel et al., 1986; Larrasoaña et al., 2004; Mattei et al., 1995, 1997; Parés, 2004; Sagnotti et al., 1998, 1999; Tarling and Hrouda, 1993), foreland basins (Parés et al., 1999; Pueyo Anchuela et al., 2010; Soto et al., 2009; Weaver et al., 2004), and accretionary prisms (Kanamatsu et al., 2001; Kissel et al., 1986; Weaver et al., 2004) through the study of weak tectonic fabrics in mudrocks that typically appear undeformed at outcrop scale. Tectonic analysis of magnetic fabrics of these so-called weakly deformed mudrocks are based on a presumed rapid overprint of deformation on initial sedimentary fabrics shortly after deposition, when mudrocks are still flat-lying, soft and the presence of water allows reorientation of mineral grains according to the prevailing stress field (Benn, 1994; Borradaile and Tarling, 1981; Parés, 2004; Richter et al., 1993). This assumption is particularly important for palaeostress determinations, which require a rapid tectonic overprint so that the magnetic ellipsoid represents the best possible approximation to the incremental strain ellipsoid (Soto et al., 2009). While rapid locking of tectonic fabrics during early burial appears to be well supported (Larrasoaña et al., 2004; Mattei et al., 1995; Parés, 2004; Parés et al., 1999; Sagnotti et al., 1999; Soto et al., 2009), the time lag between sediment deposition and imposition of the tectonic overprint, as well as the time taken for such an overprint to be effectively locked, are yet to be determined. Such quantification has been hampered by difficulties in establishing an absolute chronology for early burial processes in ancient mudrocks, on which most AMS studies have been made. Here we overcome this problem by documenting tectonic fabrics in Late Holocene muds from a tectonically active compressive setting, the Tien Shan fold-and-thrust belt in Kyrgyzstan (Central Asia) (Buslov et al., 2007; Torizin et al., 2009). The time taken by tectonic deformation to overprint the initial sedimentary fabric can be readily constrained by dating the youngest sediments that document a tectonic fabric. On the other hand, the time lag between sediment deposition and tectonic overprinting can be straightforwardly determined by dating the youngest sediments that demonstrably record locked tectonic fabrics.

2. Geological setting

Lake Issyk-Kul occupies the bottom of an E–W oriented depression located between the Kungey and Terzkey mountains in the Kyrgyz

* Corresponding author. Tel.: +34 976 555153; fax: +34 976 553358.
E-mail address: jc.larra@igme.es (J.C. Larrasoaña).

0040-1951/$ – see front matter © 2011 Elsevier B.V. All rights reserved.
doi:10.1016/j.tecto.2011.05.003

Tien Shan range (Fig. 1a). This mountain range developed as a result of the far-field effects of the ongoing collision between India and Eurasia, which has led to northwesterly-directed underthrusting of the stable Tarim block beneath the Kazakhstan shield (Buslov et al., 2007; Torizin et al., 2009). The Lake Issyk-Kul basin is filled with Cenozoic continental sediments, and lacustrine sediments have been deposited since the Oligocene (Buslov et al., 2007). The basin is bounded by south- and north-verging basement thrust units that involve Precambrian and Palaeozoic rocks of the Kungey and Terzkey mountains, respectively (Buslov et al., 2007; Torizin et al., 2009). Tectonic activity in the region started in the Oligocene and peaked within the last 3–5 Myr as inferred from apatite fission-track thermochronology and magnetostratigraphic dating of Neogene sediments (Burbank et al., 1999; Buslov et al., 2007). Ongoing deformation has led to several unconformities and displaced geomorphic surfaces within and above Quaternary sediments in the Issyk-Kul area (Bowman et al., 2004). The region is affected by frequent large magnitude (6.5–8.7) earthquakes that occur mainly on the thrust faults that separate the Lake Issyk-Kul basin from the Kungey and Terzkey ranges (Abdrakhmatov and Djanuzakov, 2002; Torizin et al., 2009) (Fig. 1a). Global positioning system (GPS) data indicate a present-day horizontal displacement that ranges between 2 and 10 mm/yr along the northern and southern shores of Lake Issyk-Kul, respectively, relative to stable Asia (Abdrakhmatov et al., 1996; Torizin et al., 2009). This horizontal displacement has occurred along a north–south shortening direction since the Pliocene–early Quaternary (Buslov et al., 2007).

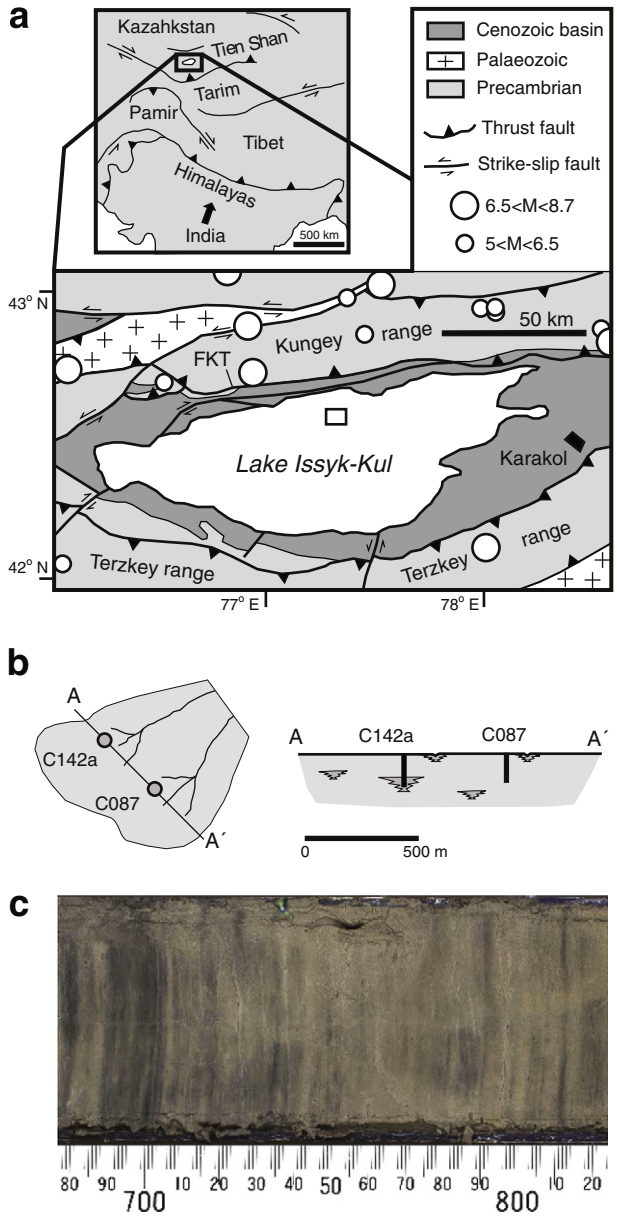

Fig. 1. Geological setting of the studied sediment cores. (a) Geological sketch map of the Lake Issyk-Kul basin and surrounding mountain ranges in the context of the India-Asia collision. FKT denotes the Fore Kungey thrust (Buslov et al., 2007). White circles indicate the location of strong historic earthquakes (Abdrakhmatov and Djanuzakov, 2002; Torizin et al., 2009). The box denotes the location, east of a reverse fault located on the NW shore of the lake, of cores C142a and C087. (b) Sketch of the location of the studied cores within a lobe of the deltaic system that drains the northern shore of Lake Issyk-Kul, in map view and cross-section. (c) Image of sediments that dominate core C087 and most of core C142a. The scale is in millimetres.

3. Materials and methods

Cores C142a (42°34′31.2″ N–77°20′03.0″ E) and C087 (42°34′5.22″ N–77°20′10.44″ E) were collected using a gravity corer at water depths of 150 and 312 m, respectively (Fig. 1a). These azimuthally unoriented cores were recovered from the upper slope of the central northern margin of Lake Issyk-Kul, just east of a reverse fault located on the NW shore of the lake. Core C142a comprises a 150-cm-thick sequence of Late Holocene clays, silts and sandy silts that accumulated on a distal lobe of the deltaic system that drains into the lake along a NE–SW direction (Fig. 1b) (see de Batist et al., 2002). The uppermost 18 cm of the core is composed of dark, organic-rich and massive silty clays. Between depths of 18 and 94 cm, the sediments consist of alternating light and dark grey clays. The lowermost 56 cm of the core consists of alternating light and dark silts and sandy silts that provide evidence for a distributary channel that supplied coarser-grained sediments to the deltaic system. Core C087 comprises 132 cm of clays and silty clays that are equivalent to those in the uppermost 94 cm of core C142a (Fig. 1c). The lack of coarser-grained sediments at the base of core C087 might be explained by the discontinuous nature of deltaic tributary systems (Fig. 1b).

Back-to-back palaeomagnetic samples were obtained by pushing 63 and 52 plastic boxes ($2\times2\times2$ cm) into the working half of cores C142a and C087, respectively. AMS measurements were conducted using an AGICO KLY-2 magnetic susceptibility meter at the Paleomagnetic Laboratory of the ICT Jaume Almera (UB-CSIC), Barcelona, Spain, using a field of 0.1 mT and a frequency of 470 Hz. The AMS is a second-rank tensor that can be graphically displayed as a three-axis ($\kappa_{max}>\kappa_{int}>\kappa_{min}$) ellipsoid with a given orientation, shape and degree of anisotropy (Tarling and Hrouda, 1993). The shape and degree of anisotropy of the magnetic ellipsoid for each sample can be described using the shape (T) and corrected anisotropy degree (P^j) parameters of Jelínek (1981), respectively. T ranges between 1 and −1 for pure oblate and prolate ellipsoids, respectively, and is about 0 for triaxial ellipsoids (Jelínek, 1981). P^j gives an idea of the strengh of the ellipsoid (Jelínek, 1981). Its value depends on the degree of anisotropy of the rock-forming minerals, and ranges between 1 and 1.15 for weakly deformed mudrocks whose magnetic susceptibility is dominated by paramagnetic minerals (Parés, 2004). Relevant AMS parameters for each sample are summarised in the supplementary data as a function of depth and age. The mean orientation of the magnetic ellipsoid for all samples and the associated confidence ellipses were calculated following Jelínek (1981).

Palaeomagnetic analyses were conducted at UB-CSIC, and involved progressive alternating field (AF) demagnetization and subsequent measurement of the natural remanent magnetization (NRM) for all samples. The NRM was measured using a 2-G Enterprises three-axis superconducting rock magnetometer, with AF demagnetization up to a maximum field of 100 mT at steps ranging between 5 and 30 mT. Stable palaeomagnetic directions were identified from orthogonal demagnetization plots (Zijderveld, 1967) and were calculated by

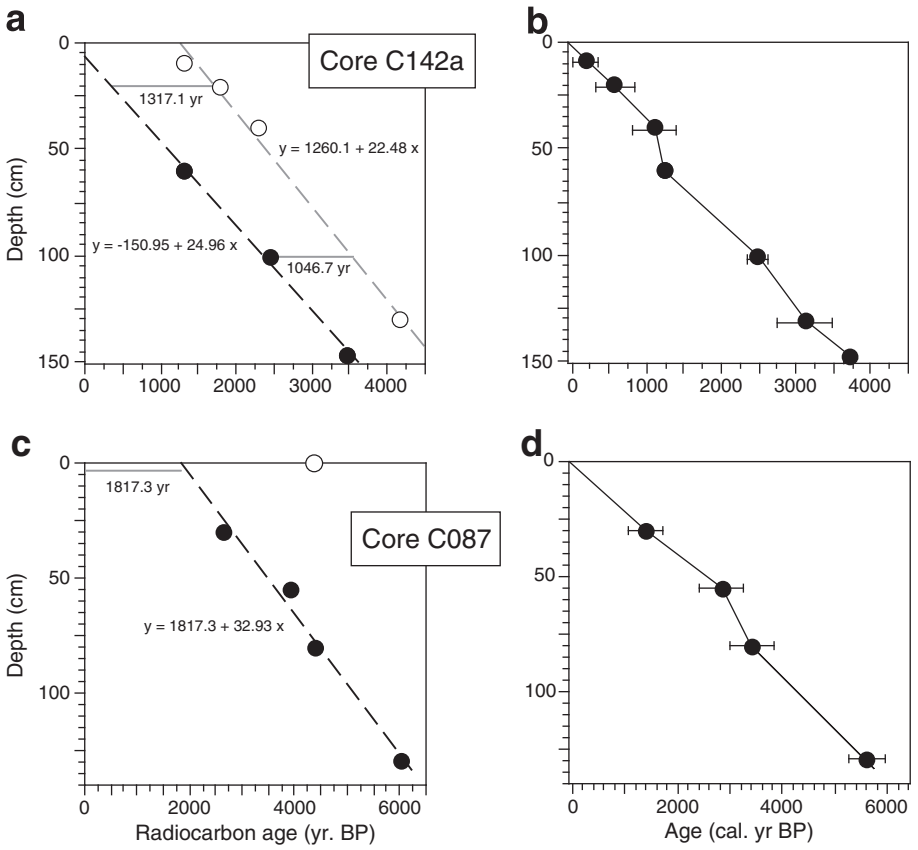

Fig. 2. Age models for cores C142a and C087. (a) Plot of depth versus radiocarbon ages for core C142a. The grey and black dashed lines represent linear fits to the samples affected (open circles) and not affected (bold circles) by a radiocarbon reservoir effect. The equations corresponding to both regressions are indicated. Grey horizontal lines correspond to the age difference between the two linear regression models calculated at depths of 20 and 100 cm. (b) Depth–age model (in calendar years) for core C142a constructed after correcting the relevant samples for a reservoir age of 1182 yr BP. Horizontal bars represent the respective 2σ errors. (c) Plot of depth versus radiocarbon ages for core C087. (d) Depth–age model (in calendar years) for core C087 constructed after correcting the relevant samples for a reservoir age of 1182 yr BP. Horizontal bars represent the respective 2σ errors.

fitting linear trends using principal component analysis (Kirschvink, 1980).

The age model for the studied sediments is based on ^{14}C dating of twelve pollen samples from throughout both cores. These samples were enriched following the procedure of Rull et al. (2010) and were dated using accelerator mass spectrometry ^{14}C dating at the Poznan Radiocarbon (http://www.radiocarbon.pl/) and Beta Analytics Inc. (http://www.radiocarbon.com/) laboratories. The radiocarbon dates were calibrated using the online software CALIB 6.0 (http://calib.qub.ac.uk/calib/) and the INTCAL09 curve (Reimer et al., 2009).

X-ray diffraction and hysteresis analyses of sediments from core C142a were performed to determine the mineralogical source of magnetic fabrics in the studied sediments. X-ray diffraction analyses were performed for samples taken at 1-cm intervals using an automatic Siemens D-500 X-ray diffractometer at the ICT Jaume Almera (CSIC). The diffractometer is equipped with a graphite monochromator and operates with a Cu kα source at 40 kV and 30 mA. Hysteresis measurements for every fourth sample were made using a Princeton Measurements Corporation vibrating sample magnetometer at the Kochi Core Center, Japan, up to maximum fields of 1 T to enable calculation of the relative contribution of paramagnetic and ferrimagnetic minerals to the low-field magnetic susceptibility (Hrouda and Jelínek, 1990). We estimated the percentage paramagnetic contribution by comparing the high-field slope of hysteresis loops (at ~1 T) with the total susceptibility (the bulk magnetization at 1 T normalised by the same field). The ferrimagnetic contribution equals the total susceptibility minus the paramagnetic contribution.

4. Results

4.1. Core C142a

The ^{14}C age–depth relationship of samples from Core C142a contains age reversals at depths of 130 cm and above 40 cm (Fig. 2a) (Table 1). Closer inspection reveals that the samples are arranged in two groups. The ages of samples at depths of 60, 100, and 147 cm lie on a line ($R^2 = 0.996$) that nearly intercepts the core top (Fig. 2a). In contrast, the other group of samples has ^{14}C ages that lie along a line ($R^2 = 0.995$) that intercepts the core top at ca 1260 ^{14}C yr BP (Fig. 2a). The lines are nearly parallel, so that the time difference between the linear models at depths of 20 cm and 100 cm is 1317 and 1047 yr, respectively. The most likely explanation for the older ages of the second group of samples is that they are affected by a reservoir effect linked to the presence of old carbon-bearing aquatic pollen remains, which have been demonstrated to include *Botryoccocus* sp. in a core located close to core C142a (Giralt et al., 2004). An alternative explanation, involving reworking of organic matter from older lacustrine and/or terrestrial sediments, is unlikely because there is no sedimentological evidence for reworking and, even if this was the case, a less systematic age effect would be expected rather than the observed constant offset.

By averaging the time difference between the fitted lines for the two groups of samples, a mean reservoir age of 1182 ± 135 ^{14}C yr BP can be estimated for the studied Issyk-Kul sediments. This value is consistent, especially considering potential changes in reservoir effect linked to a number of variables (Gouramanis et al., 2010; Wu et al.,

Table 1
Accelerator mass spectrometer radiocarbon dates used to construct the age models for cores C142a and C087.

Core	Sample depth (cm)	Laboratory number	Dated material	Radiocarbon age (yr. BP)	Reservoir effect (yr. BP)[1]	Calibrated age (cal.yr. BP)[2]
C142a	9	Poz-32009	Pollen-enriched extract	1300 ± 30	1182 ± 135	171 ± 171
	20	Poz-35814	Pollen-enriched extract	1790 ± 30	1182 ± 135	569 ± 264
	40	Poz-35813	Pollen-enriched extract	2280 ± 30	1182 ± 135	1101 ± 289
	60	Poz-32073	Pollen-enriched extract	1290 ± 35	0	1232 ± 62
	100	Poz-32008	Pollen-enriched extract	2450 ± 50	0	2488 ± 131
	130	Poz-35815	Pollen-enriched extract	4145 ± 35	1182 ± 135	3116 ± 362
	147	Poz-32074	Pollen-enriched extract	3470 ± 40	0	3739 ± 101
C087	0	Beta-295531	Pollen-enriched extract	4360 ± 30	1182 ± 135	3350 ± 390[3]
	30	Beta-295532	Pollen-enriched extract	2630 ± 30	1182 ± 135	1380 ± 330
	55	Beta-295533	Pollen-enriched extract	3910 ± 30	1182 ± 135	2840 ± 410
	80	Beta-295534	Pollen-enriched extract	4380 ± 30	1182 ± 135	3410 ± 420
	129	Beta-295536	Pollen-enriched extract	6030 ± 40	1182 ± 135	5600 ± 340

[1] The reservoir effect inferred for each sample.
[2] Ages in calendar years, along with the associated 2σ error after subtracting the reservoir effect and calibrating the resulting age.
[3] Rejected date.

2010), with the 840 ± 35 ^{14}C yr BP age established on the basis of dated adult ostracods from the uppermost (2.5 cm) sediments of Lake Issyk-Kul (Ricketts et al., 2001). This estimated value is also similar to the reservoir effect established for other large central Asian lakes such as Lake Baikal, which ranges between 1130 and 1588 ^{14}C yr BP in different cores (Prokopenko et al., 2007).

After correcting the radiocarbon ages of the relevant samples for the mean estimated 1182 ± 135 ^{14}C yr BP reservoir age, we constructed an age model for core C142a by using calibrated ages chosen on the basis of their maximum probability distribution within the 2σ interval (Table 1). The corrected age model (Fig. 2b) is based on linear interpolation between calibrated radiocarbon dates, and assumes a 2000 yr AD age for the top of the core. Such an assumption is validated by ^{210}Pb and ^{137}Cs ages of core top sediments studied previously in Lake Issyk-Kul in the vicinity of core C142a (Giralt et al., 2002, 2004). The corrected age model gives steady accumulation rates throughout core C142a, and indicates that its sedimentary record includes the last ca 3800 cal.yr BP.

The low-field magnetic susceptibility of the studied sediments from core C142a ranges between 200 and 500×10^{-6} SI in the uppermost 94 cm of the studied core, and rapidly increases to almost 2000×10^{-6} SI below that depth (supplementary data). Magnetic hysteresis data demonstrate that samples with bulk susceptibilities lower than 500×10^{-6} SI have a dominant contribution from paramagnetic minerals (average paramagnetic contribution = 63.6 ± 4%), whereas higher susceptibilities are linked to a predominant ferrimagnetic contribution (average paramagnetic contribution = 37.7 ± 10.9%) (Fig. 3a) (supplementary data), which is most likely magnetite. This contrasting behaviour appears to be caused by a coarser sediment texture below 94 cm and a concomitant increase in concentration of ferrimagnetic minerals. X-ray diffraction analyses indicate that the main paramagnetic minerals in these sediments are illite (average content = 29.7 ± 8.6%) and clinochlorite (average content = 15.4 ± 3.7%) (Fig. 3b), which indicates that the magnetic fabric of the paramagnetic-dominated samples is due to the preferred orientation of these two phyllosilicates. The radiocarbon-based age model enables examination of relevant AMS parameters as a function of age (Fig. 4) (supplementary data). Coarser ferrimagnetic-dominated sediments are characterized by P^j values that range between 1.15 and 1.3 and by T values that range between 0.4 and 0.95, which indicate strong triaxial to oblate fabrics (Jelínek, 1981). The magnetic fabric of the ferrimagnetic-dominated sediments is characterized by the tight cluster of minimum susceptibility (κ_{min}) axes around the pole to bedding, and by the alignment of maximum susceptibility (κ_{max}) axes at an oblique angle with respect to the push direction during sampling (Fig. 5a). Fine-grained paramagnetic-dominated sediments are charaterized by P^j values that range between 1.02 and 1.13 and by T values that range between −0.41 and 0.82, which indicate weaker prolate to oblate fabrics (Jelínek, 1981). The magnetic fabric of paramagnetic-dominated sediments is characterized by tightly clustered maximum susceptibility (κ_{max}) axes around a direction that is slightly oblique, considering error estimates, to the push direction (Fig. 5b). Minimum susceptibility (κ_{min}) axes are distributed along a well-developed girdle perpendicular to the mean of the κ_{max} axes, with the mean κ_{min} aligned with the pole to bedding. This type of fabric does not conform to a classic compaction-driven sedimentary fabric, in which the random deposition of platy phyllosilicates within the bedding plane gives way to a scattering of κ_{max} axes within the bedding plane (Benn, 1994; Parés, 2004; Sintubin, 1994), but to a tectonic fabric with a well-developed magnetic lineation (Aubourg et al., 1995; Cifelli et al., 2009; Kanamatsu et al., 2001; Kissel et al., 1986; Kligfield et al., 1981; Larrasoaña et al., 2004; Mattei et al., 1995, 1997; Parés, 2004; Parés et al., 1999; Sagnotti et al., 1998, 1999; Soto et al., 2009; Tarling and Hrouda, 1993; Weaver et al., 2004).

Stepwise AF demagnetization of all the studied samples reveals a single stable remanence component that is directed toward the origin of demagnetization plots (Fig. 6a). The mean declination of this characteristic remanent magnetization (ChRM) (supplementary data) is deviated 6.9° counter-clockwise from the mean expected geomagnetic field declination in the studied area for the same time interval (ca 3800 yr BP) (Korte and Constable, 2005) (Fig. 6b). The mean palaeomagnetic inclination of the ChRM is 35.5°, which is 22.5° shallower than the expected value (58.0°) for the studied area (Korte and Constable, 2005). It appears that, in addition to the potential inclination error associated with acquisition of a depositional remanent magnetization (King, 1955; Tauxe, 2005), processes such as coring-induced compaction might be required to explain such strong inclination flattening.

4.2. Core C087

The ^{14}C age–depth relationship of samples from core C087 contains no age reversals, although the age for a sample from the top of the core has been rejected (Table 1, Fig. 2c). The remaining four samples lie on a line ($R^2 = 0.99$) that intercepts the core top at 1817.3 ^{14}C yr BP. After correcting these samples for the 1182 ± 135 ^{14}C yr BP reservoir age estimated from core C142a, these ages lie on a line that intercepts the core top at 263 cal. yr BP (Fig. 2d). This value is consistent, keeping in mind the 2σ interval of the radiocarbon dates, with a 2000 yr AD age for the top of the core, which validates the 1182 ± 135 ^{14}C yr BP reservoir age estimated from core C142a.

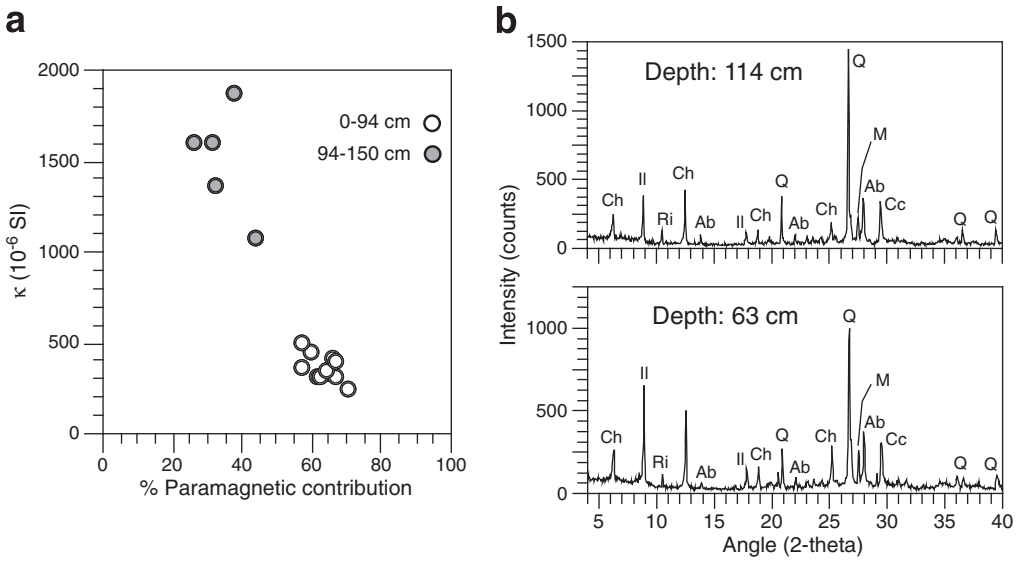

Fig. 3. Mineralogical source of the magnetic fabrics for the studied sediments. (a) Plot of the percentage paramagnetic contribution to the bulk magnetic susceptibility versus bulk susceptibility for core C142a sediments (κ). (b) X-ray diffractograms for representative samples (depths of 63 and 114 cm) from core C142a. Ch: clinochlorite; Il: illite; Q: quartz; Cc: calcite; Ab: albite; Ri: riebeckite; and M: microcline.

The corrected age model (Fig. 2d) is based on linear interpolation between the four calibrated radiocarbon dates, and assumes a 2000 yr AD age for the top of the core. This age model indicates steady accumulation rates throughout core C087, whose sedimentary record encompasses the last ca 5600 cal. yr BP.

The low-field magnetic susceptibility of sediments from this core oscillates around 235×10^{-6} SI and has maximum values of 388×10^{-6} SI (supplementary data), which indicates a dominant contribution of paramagnetic minerals to the AMS. Sediments from core C087 are characterized by P^j values that range between 1.03 and 1.15 and by T values that range between 0.26 and 0.98 (supplementary data), which indicate weak triaxial to strong oblate fabrics (Jelínek, 1981). Their magnetic fabric is characterized by a tight clustering of κ_{min} axes around the pole to bedding. κ_{max} axes appear scattered within the bedding plane, but have weak clustering around a mean direction that is more than 60° away from the perpendicular to the push direction (Fig. 7a).

Samples from core C087 have the same ChRM coercivity spectra as samples from core C142a (Fig. 7b). The mean ChRM declination (supplementary data) is deviated 28.9° clockwise from the mean expected geomagnetic declination in the area for the same time interval (Korte and Constable, 2005) (Fig. 7c). The mean ChRM inclination of 50.6° is much closer to the expected value (58.3°) for the studied area (Korte and Constable, 2005) than that for core C142a.

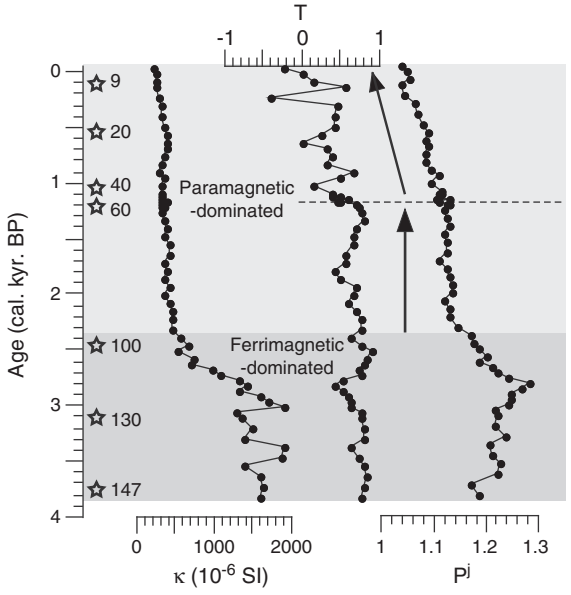

Fig. 4. Variations of relevant AMS parameters of core C142a as a function of age. Stars mark the position (in cm) of seven ^{14}C samples used to construct the age model (as shown in Fig. 2).

5. Discussion

Pushing plastic boxes into sediment cores during sampling can induce a weak, spurious fabric that is characterized by development of a magnetic lineation perpendicular to the push direction during sampling (Copons et al., 1997). The magnetic lineation of sediments from core C087 and of both the ferrimagnetic- and paramagnetic-dominated sediments of core C142a is oblique, with variable angles, with respect to the push direction (Figs. 5 and 6). Moreover, the magnetic ellipsoid shape for sediments from cores C142a and C087 is different. Both cores were sampled following exactly the same procedure, which provides evidence against sampling-induced fabrics and indicates that the studied paramagnetic-dominated fabrics are genuine tectonic fabrics.

Further evidence for genuine tectonic fabrics is provided by examining the directional attributes of the magnetic ellipsoids when the cores are rotated back to their initial position using palaeomagnetic data. After subtracting −6.9° and 28.9° from the paramagnetic-dominated fabrics of cores C142a and C087, respectively, the mean κ_{max} directions become parallel, within error estimates, to the trend of the neighbouring Fore Kungey thrust (Figs. 6c, d and 7d). The rotated mean κ_{max} directions are also perpendicular to the mean present-day shortening direction in the area as derived from GPS data (Buslov et al., 2007; Torizin et al., 2009) (Fig. 6c and 7d). Moreover, the girdle of κ_{min} orientations observed for core C142a becomes parallel to the shortening direction (Buslov et al., 2007; Torizin et al., 2009) and perpendicular to the Fore Kungey thrust (Fig. 6c). In the case of the ferrimagnetic-dominated sediments of core C142a, subtracting −6.9° from their fabrics results in a mean κ_{max} that becomes strikingly parallel, within error estimates, to the direction of the distributary

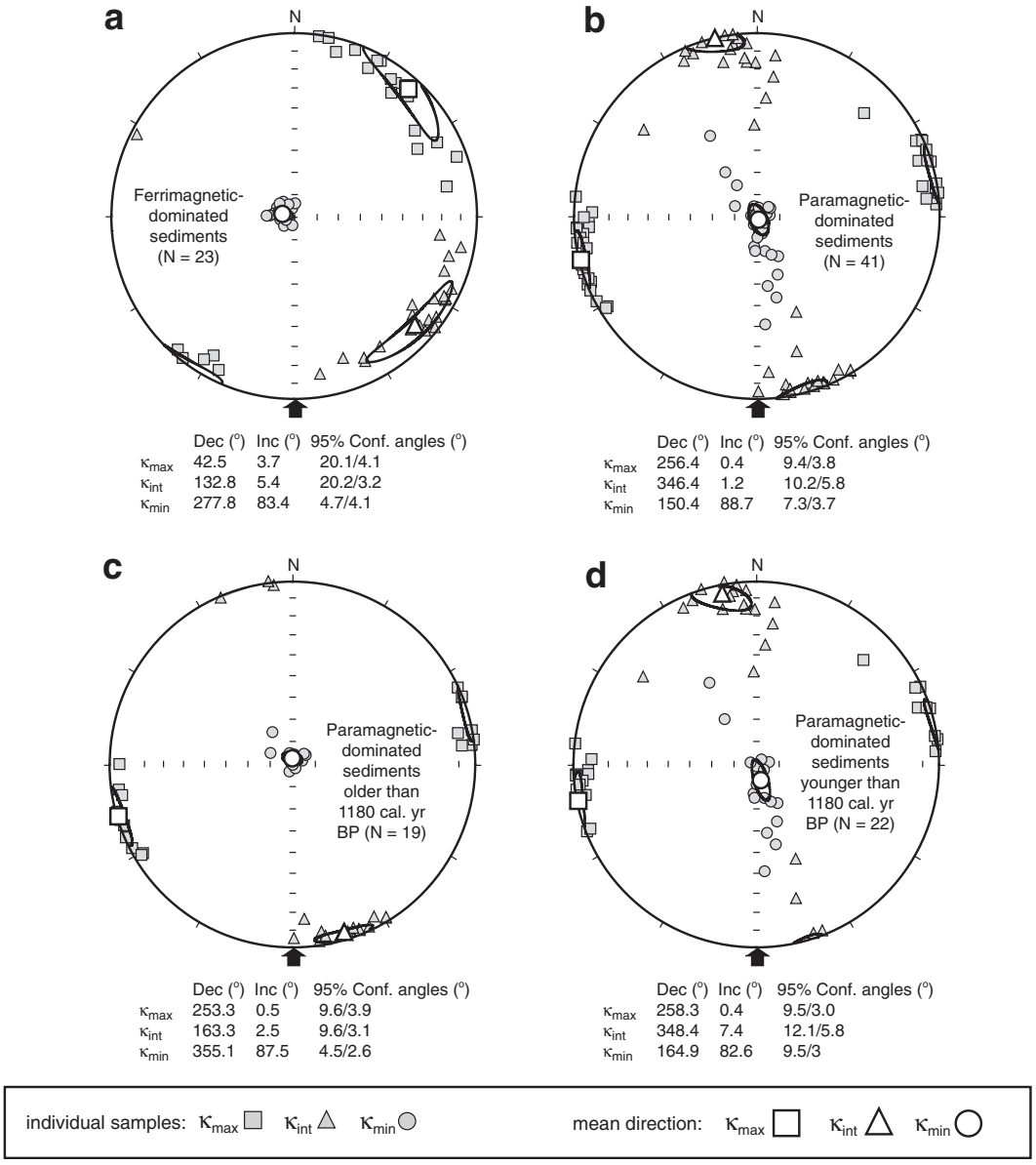

Fig. 5. Equal area stereographic projections (in core coordinates) of AMS data from core C142a. (a) For ferrimagnetic-dominated sediments. (b) For all paramagnetic-dominated sediments. (c) For paramagnetic-dominated sediments older than 1180 cal. yr BP. (d) For paramagnetic-dominated sediments younger than 1180 cal. yr BP. κ_{max}, κ_{int} and κ_{min} axes of individual samples are depicted using small grey squares, triangles and circles, respectively. For each dataset, the mean directions of the κ_{max}, κ_{int} and κ_{min} axes are depicted using large white squares, triangles and circles, respectively, and are shown along with their 95% confidence ellipses. The black arrows indicate the push direction during sampling. N denotes the number of samples for each dataset.

channels of the deltaic system from which core C142a was collected (Fig. 6d). This indicates that the ferrimagnetic-dominated fabrics are controlled by the effect of palaeocurrents on the orientation of magnetite grains rather than by tectonic deformation. Tectonic strain therefore appears to have overprinted the initial sedimentary fabric of the paramagnetic-dominated sediments, but not that of the ferrimagnetic-dominated sediments. This suggests that the much larger (typically tens to hundreds of microns) and platy paramagnetic phyllosilicate minerals are more susceptible to imposition of a tectonic fabric than ferrimagnetic grains (which are typically submicron to a few microns in size).

The documented magnetic fabrics from cores C142a and C087 are identical to those that are typical of mudrocks that have undergone initial tectonic compression (Aubourg et al., 1995; Borradaile and Tarling, 1981; Cifelli et al., 2009; Graham, 1954, 1967; Kanamatsu et al., 2001; Kissel et al., 1986; Kligfield et al., 1981; Larrasoaña et al., 2004; Mattei et al., 1995, 1997; Parés, 2004; Parés et al., 1999; Sagnotti et al., 1998, 1999; Soto et al., 2009; Tarling and Hrouda, 1993; Weaver et al., 2004). This type of fabric results from the overprint of tectonic strain on an initial sedimentary fabric, where random deposition of platy phyllosilicate grains within the bedding plane gives way to development of a strongly oblate compaction-driven magnetic fabric (Benn, 1994; Parés, 2004; Sintubin, 1994). Initial deformation drives incipient rotation of phyllosilicates within the bedding plane, away from the shortening direction and around their long axis. Phyllosilicates therefore begin to develop an intersection lineation that is marked by an incipient clustering of κ_{max} axes and results in a subtle, yet significant, magnetic lineation that is broadly perpendicular to the shortening direction (Larrasoaña et al., 2004; Parés, 2004; Parés and van der Pluijm, 2002). Further deformation enhances rotation of phyllosilicates so that their intersection lineation is strengthened. This process leads to an enhanced magnetic lineation and to improved clustering of mean κ_{max} axes perpendicular to the shortening direction (Larrasoaña et al., 2004; Parés, 2004; Parés and

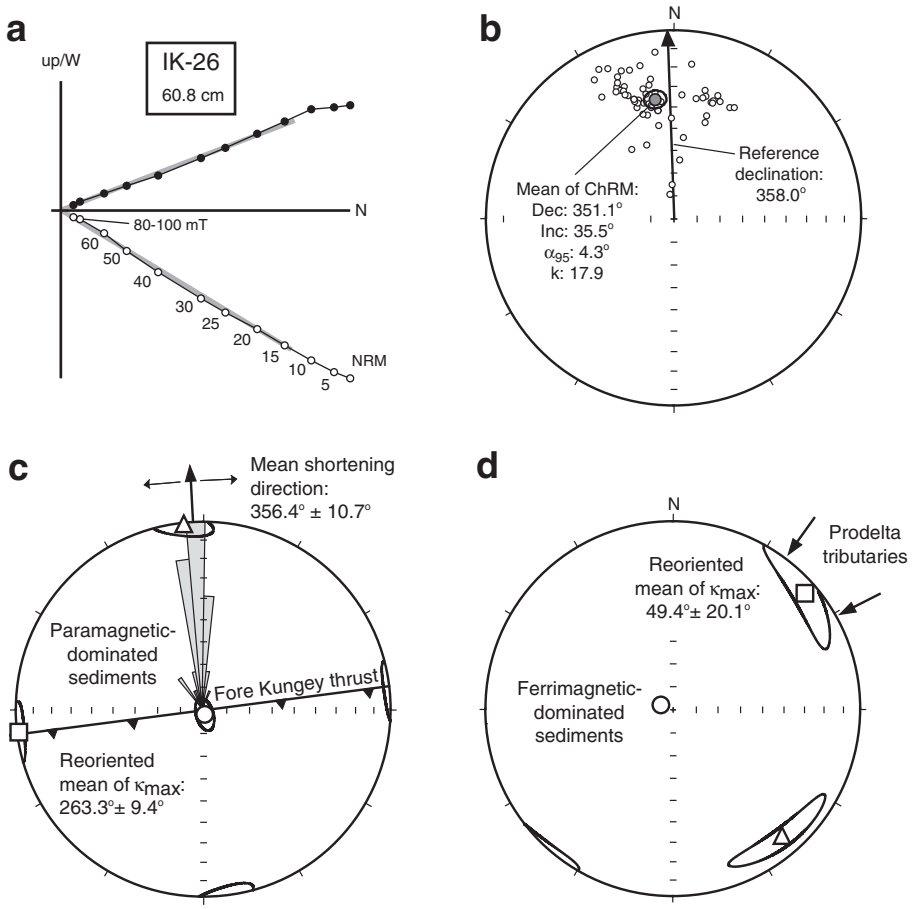

Fig. 6. Palaeomagnetic correction of AMS data for core C142a. (a) Representative orthogonal demagnetization diagram for the studied samples (plotted in core coordinates). The grey lines represent the linear fit to the ChRM direction, which was isolated between 15 and 80–100 mT for all studied samples. (b) Equal area stereographic projection of ChRM directions in core coordinates, plotted with the mean direction and reference declination for the studied area for the last ca 3800 yr BP (Korte and Constable, 2005). (c) Equal area stereographic projection of palaeomagnetically corrected AMS data for all paramagnetic-dominated sediments, plotted with GPS-derived shortening directions around Lake Issyk-Kul (Torizin et al., 2009) and the trend of the neighbouring Fore Kungey thrust (Buslov et al., 2007; Torizin et al., 2009). GPS-derived directions are plotted in a rose diagram (using 5° intervals) whose maximum radius represents 30% of the total data set (N = 33). The angle between the mean shortening direction and the perpendicular to the mean of the κ_{max} axes is 3.1°, which is well within the error associated with both mean directions. (d) Equal area stereographic projection of palaeomagnetically corrected AMS data for the ferrimagnetic-dominated sediments, plotted with the orientation of the main tributaries of the deltaic system from which core C142a was collected.

van der Pluijm, 2002). Increased deformation enhances rotation of phyllosilicates around their long axes so that κ_{min} axes begin to girdle around tightly clustered κ_{max} axes. This fabric development is accompanied by a decreased degree of anisotropy (from initial values down to $P^j<1.1$) and by a change in magnetic ellipsoid shape from oblate ($T>0$) to triaxial ($T\sim0$) and eventually to prolate ($T<0$) (Parés, 2004; Tarling and Hrouda, 1993).

Sediments from core C087 are characterized mainly by well-developed oblate fabrics ($1.03<P^j<1.15$; $0.26<T<0.98$), with κ_{min} axes that are tightly clustered around the pole to bedding and κ_{max} axes that are weakly clustered broadly parallel to the trend of the neighbouring structures (Fig. 7c). These fabrics correspond to the onset of the so-called "earliest deformation" stage of petrofabric development reported in mudrocks undergoing initial deformation (Parés, 2004; Parés et al., 1999; Ramsay and Huber, 1983). In core C142a, paramagnetic-dominated sediments before and after ca 1180 cal. yr BP have magnetic ellipsoids with identical directional properties but with different shapes and degrees of anisotropy. Before 1180 cal. yr BP, well-developed oblate to triaxial fabrics ($1.1<P^j<1.13$; $0.44<T<0.82$) (Fig. 4) have κ_{min} and κ_{max} axes tightly clustering around the pole to bedding and the trend of the neighbouring structures, respectively (Fig. 5c). After 1180 cal. yr BP, sediments are characterized by weaker triaxial to prolate fabrics ($1.03<P^j<1.12$; $-0.41<T<0.68$) (Fig. 4) in which κ_{min} axes girdle around κ_{max} axes, which are tightly clustered around the trend of the neighbouring structures (Fig. 5d). These fabrics observed before and after 1180 cal. yr BP correspond to the "earliest deformation" and "pencil structure" stages, respectively, of petrofabric development in weakly deformed mudrocks (Parés, 2004; Parés et al., 1999; Ramsay and Huber, 1983). These results provide unequivocal evidence for a tectonic origin of the documented magnetic fabrics in the Late Holocene Lake Issyk-Kul sediments. The change from "earliest deformation" to "pencil structure" fabrics observed in core C142a after 1180 cal. yr BP suggests an increase in strain conditions in the Issyk-Kul area after that age. Palaeoseismic data from the Issyk-Kul area extend back to 1500 yr BP (Torizin et al., 2009). Unfortunately, large gaps in the palaeoseismic record before 200 yr BP preclude testing of the possibility of increased strain after 1180 cal. yr BP.

Several studies have demonstrated that magnetic fabrics of sediments located in the vicinity of compressive faults (e.g. Larrasoaña et al., 2004; Mattei et al. 1997; Parés et al., 1999), even with minor horizontal displacements of <2 m (Soto et al., 2009), often have a stronger tectonic overprint than those located at greater distances from faults. Cores C087 and C142a were recovered from the upper slope of the central northern margin of Lake Issyk-Kul, east of a reverse fault located on the NW shore of the lake (Fig. 1). The overall weaker tectonic overprint of sediments from core C087 compared to those of core C142a can therefore be easily explained by its closer location to neighbouring

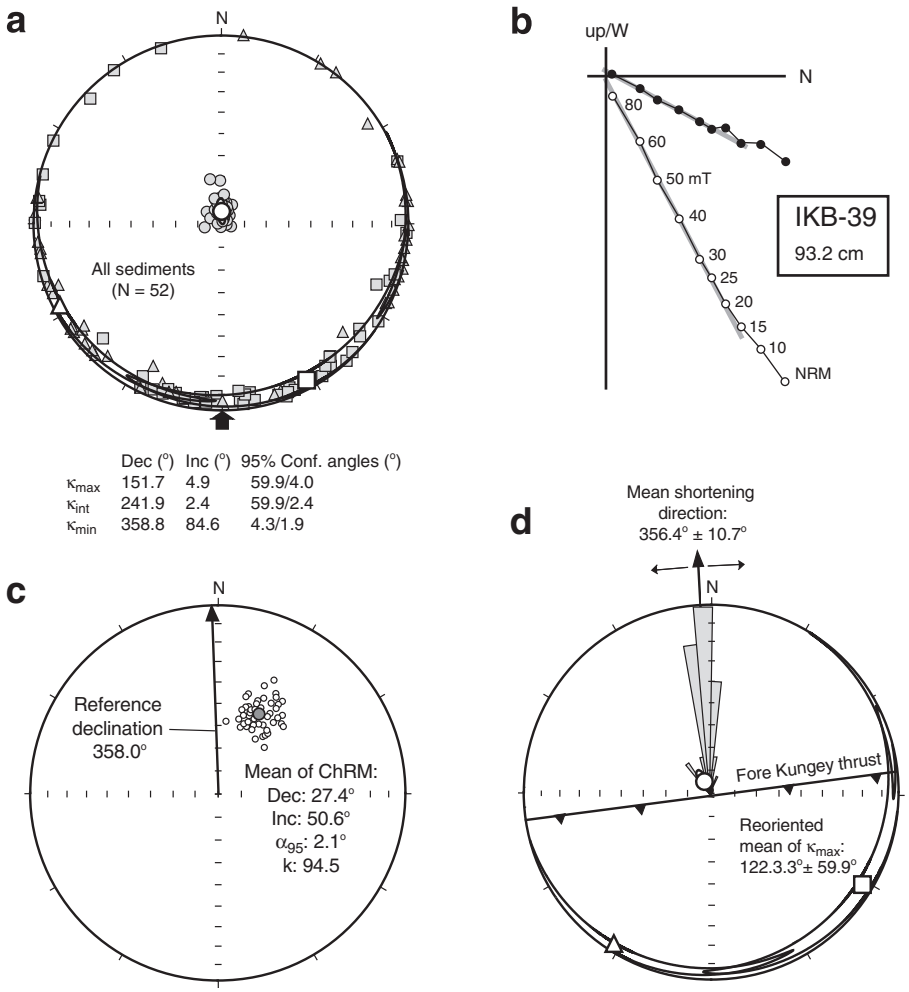

Fig. 7. Palaeomagnetic correction of AMS data for core C087. (a) Equal area stereographic projection of AMS data for core C087. (b) Representative orthogonal demagnetization diagram for the studied samples (plotted in core coordinates). (c) Equal area stereographic projection of ChRM directions in core coordinates, plotted with the mean direction and reference declination for the studied area for the last ca 5600 yr BP (Korte and Constable, 2005). (d) Equal area stereographic projection of palaeomagnetically corrected AMS data for core C087, plotted with GPS-derived shortening directions around Lake Issyk-Kul (Torizin et al., 2009) and the trend of the neighbouring Fore Kungey thrust (Buslov et al., 2007; Torizin et al., 2009). Symbols are as in Figs. 5 and 6.

small-scale active faults. Although seismic profiles point to a fault-dominated configuration of the lake floor area where the studied cores were collected, unfortunately they do not have enough resolution and penetration to image such faults (de Batist et al., 2002).

Our chronology for core C142a indicates that sediments as young as 25 yr have well-developed tectonic fabrics (Figs. 4 and 5, supplementary data). Moreover, the fact that sediments older than 1180 cal.yr BP record a weaker tectonic overprint than younger sediments (Figs. 4 and 5) indicates that their fabrics are effectively locked and that they have not recorded the subsequent increase in tectonic deformation after 1180 cal.yr BP. The apparent increase in tectonic overprint after 1180 cal.yr BP might be caused by the higher plasticity of the uppermost, less compacted sediments, which could lead to an artificial strengthening of the fabric during sampling. However, the lack of a change in orientation of the magnetic ellipsoid at around 1180 cal.yr BP makes this possibility unlikely. Overall, our results provide the first firm indication not only for extremely rapid (i.e., 25 yr) overprinting of tectonic fabrics in mudrocks, but also for their rapid (i.e., ~1 kyr) effective locking. Importantly, potential radiocarbon dating errors of the order of 1 kyr do not influence significantly our estimates of the locking time of the studied tectonic fabrics. Our results therefore validate the suitability of weak tectonic fabrics for unravelling deformation mechanisms, palaeostress directions and the kinematic evolution of compressive settings such as fold-and-thrust belts, accretionary prisms and foreland basins during initial deformation. Future AMS studies of modern sediments from tectonically active regions could therefore open new opportunities for tectonic applications of magnetic fabrics by providing quantitative insights into the elusive relationship between magnetic ellipsoids, shortening rates, and stress directions, which can then provide constraints on deformation mechanisms.

6. Conclusions

Our results demonstrate that Late Holocene sediments from Lake Issyk-Kul, in which magnetic fabrics reflect the preferred orientation of phyllosillicates, have tectonic magnetic fabrics identical to those recorded by mudrocks that have undergone initial tectonic compression. The mean orientation of the susceptibility maxima parallels neighbouring active thrust faults and is perpendicular to the geodetically-derived local shortening direction. The radiocarbon-based age model for core C142a indicates that sediments as young as 25 yr record this clear tectonic fabric, which is locked within sediments older than 1180 cal.yr BP. These results provide the first quantitative demonstration of rapid locking of tectonic fabrics of weakly deformed mudrocks shortly after deposition. Our observations validate the reliability of AMS analyses for unravelling initial deformation conditions in compressive settings. Future AMS studies

of recent sediment from active tectonic settings could therefore open new opportunities for providing quantitative insights into the relationship between magnetic ellipsoids, shortening rates, and stress directions in compressive settings.

Supplementary materials related to this article can be found online at doi:10.1016/j.tecto.2011.05.003.

Acknowledgements

Financial support for this research was provided by a CSIC JAE-Doc post-doctoral research contract (MGP) and the GRACCIE (Spanish Consolider-Ingenio CSD2007-00067) and APELIK (EUICA2-CT-2000-10003) research projects. We are grateful to Jewgenij Torizin and Marc de Batist, who provided us with the palaeoseismological data set for the Lake Issyk-Kul region and the seismic profiles of the coring area, respectively. We are also indebted to Don Tarling and two anonymous reviewers, whose constructive criticisms greatly improved this paper.

References

Abdrakhmatov, K.E., Djanuzakov, K.D., 2002. Active tectonics and seismic hazard of the Issyk-Kul basin in the Kyrgyz Tien-Shan. In: Klerkx, J., Imanackunov, B. (Eds.), Lake Issyk-Kul: Its natural environment.: NATO ASI SERIES, IV. Kluwer Academic Publishers. Earth and Environmental Sciences 13, 147–160

Abdrakhmatov, K.E., Aldazhanov, S.A., Hager, B.H., Hamburger, M.W., Herring, T.A., Kalabaev, K.B., Makarov, V.I., Molnar, P., Panasyuk, S.V., Prilepin, M.T., Reilinger, R.E., Sadybakasov, I.S., Souter, B.J., Krapeznikov, Y.A., Tsurkov, V.Y., Zubovich, A.V., 1996. Relatively recent construction of the Tien Shan inferred from GPS measurements of present-day crustal deformation rates. Nature 384, 450–453.

Aubourg, C., Rochette, P., Bergmüller, F., 1995. Composite magnetic fabric in weakly deformed black shales. Physics of the Earth and Planetary Interiors 87, 267–278.

Benn, D.I., 1994. Fabric shape and the interpretation of sedimentary fabric data. Journal of Sedimentary Research 64, 910–915.

Borradaile, G.J., Henry, B., 1997. Tectonic applications of magnetic susceptibility and its anisotropy. Earth Science Reviews 42, 49–93.

Borradaile, G.J., Jackson, M., 2004. Anisotropy of magnetic susceptibility (AMS): magnetic petrofabrics of deformed rocks. In: Martín-Hernández, F., Lüneburg, C.M., Aubourg, C., Jackson, M. (Eds.), Magnetic Fabric: Methods and Applications.: Special Publication, 238. Geological Society, London, pp. 299–360.

Borradaile, G.J., Jackson, M., 2010. Structural geology, petrofabrics and magnetic fabrics (AMS, AARM, AIRM). Journal of Structural Geology 32, 1519–1551.

Borradaile, G.J., Tarling, D.H., 1981. The influence of deformation mechanisms on magnetic fabrics in weakly deformed rocks. Tectonophysics 77, 151–168.

Bowman, D., Korjenkov, A., Porat, N., Czassny, B., 2004. Morphological response to Quaternary deformation at an intermontane basin piedmont, the northern Tien Shan, Kyrgyzstan. Geomorphology 63, 1–24.

Burbank, D.W., McLean, J.K., Bullen, M., Abdrakhmatov, K.Y., Miller, M.M., 1999. Partitioning of intramontane basins by thrust-related folding, Tien Shan, Kyrgyzstan. Basin Research 11, 75–92.

Buslov, M.M., De Grave, J., Bataleva, E.A.V., Batalev, V.Y., 2007. Cenozoic tectonic and geodynamic evolution of the Kyrgyz Tien Shan Mountains: a review of geologic, thermochronological and geophysical data. Journal of Asian Earth Sciences 29, 205–214.

Cifelli, F., Mattei, M., Chadima, M., Lenser, S., Hirt, A.M., 2009. The magnetic fabric in "undeformed clays": AMS and neutron texture analyses from the Rif Chain (Morocco). Tectonophysics 466, 79–88.

Copons, R., Parés, J.M., Dinarès-Turell, J., Bordonau, J., 1997. Sampling induced AMS in soft sediments: a case study in Holocene glaciolacustrine rhythmites from Lake Barrancs (Central Pyrenees, Spain). Physics and Chemistry of the Earth 22, 137–141.

De Batist, M., Imbo, Y., Vermeesch, P., Klerkx, J., Giralt, S., Delvaux, D., Lignier, V., Beck, C., Kalugin, I., Abdrakhmatov, K.E., 2002. Bathymetry and sedimentary environments of Lake Issyk-Kul, Kyrgyz Republic (Central Asia): a large, high-altitude, tectonic lake. In: Klerkx, J., Imanackunov, B. (Eds.), Lake Issyk-Kul: Its natural environment: NATO ASI SERIES, IV. Earth and Environmental Sciences, 13, 101–123.

Giralt, S., Klerkx, J., Riera, S., Julia, R., Lignier, V., Beck, C., De Batist, M., Kalugin, I., 2002. Recent paleoenvironmental evolution of Lake Issyk-Kul. In: Klerkx, J., Imanackunov, B. (Eds.), Lake Issyk-Kul: Its natural environment: NATO ASI SERIES, IV. Earth and Environmental Sciences, 13, 125–146

Giralt, S., Julia, R., Klerkx, J., Riera, S., Leroy, S., Buchaca, T., Catalan, J., De Batist, M., Beck, C., Bobrov, V., Gavshin, V., Kalugin, I., Sukhorukov, F., Brennwald, M., Kipfer, R., Peeters, F., Lombardi, S., Matychenkov, V., Romanovsky, V., Podsetchine, V., Voltattorni, N., 2004. 1,000-years of environmental history of Lake Issyk-Kul. In: Nihoul, J.C.J., Zavialov, P.O., Micklin, P.P. (Eds.), Dying and Dead Seas: Climatic Versus Anthropic Causes.: NATO ASI SERIES, IV. Kluwer Academic Publishers. Earth and Environmental Sciences, 36, 228–253.

Gouramanis, C., Wilkins, D., De Deckker, P., 2010. 6000 years of environmental changes in Blue Lake, South Australia, based on ostracod ecology and valve chemistry. Palaeogeography, Palaeoclimatology, Palaeoecology 297, 223–237.

Graham, J.W., 1954. Magnetic susceptibility anisotropy, an unexploited petrofabric element. Bulletin of the Geological Society of America 65, 1257–1258.

Graham, J.W., 1967. Significance of magnetic anisotropy in Appalachian sedimentary rocks. In: Steinhart, J.S., Smith, T.J. (Eds.), The Earth Beneath the Continents.: Geophysical Monograph, 10. American Geophysical Union, pp. 627–648.

Hrouda, F., Jelínek, V., 1990. Resolution of ferromagnetic and paramagnetic anisotropies, using combined low-field and high-field measurements. Geophysical Journal International 103, 75–84.

Jelínek, V., 1981. Characterization of the magnetic fabric of rocks. Tectonophysics 79, 63–70.

Kanamatsu, T., Herrero-Bervera, E., Taira, A., 2001. Magnetic fabrics of soft-sediment folded strata within a Neogene accretionary complex, the Miura group, central Japan. Earth and Planetary Science Letters 187, 333–343.

King, R.F., 1955. The remanent magnetism of artificially deposited sediments. Monthly Notes of the Royal Astronomical Society. Geophysical Supplement 7, 115–134.

Kirschvink, J.L., 1980. The least-squares line and plane and the analysis of palaeomagnetic data. Geophysical Journal of the Royal Astronomical Society 62, 699–718.

Kissel, C., Barrier, E., Laj, C., Lee, T.Q., 1986. Magnetic fabric in 'undeformed' marine clays from compressional zones. Tectonics 5, 769–781.

Kligfield, R., Owens, W.H., Lowrie, W., 1981. Magnetic susceptibility anisotropy, strain, and progressive deformation in Permian sediments from the Maritime Alps (France). Earth and Planetary Science Letters 55, 181–189.

Korte, M., Constable, C.G., 2005. Continuous geomagnetic field models for the past 7 millennia: 2. CALS7k. Geochemistry, Geophysics, Geosystems 6, Q02H16. doi:10.1029/2004GC000800.

Larrasoaña, J.C., Pueyo, E.L., Parés, J.M., 2004. An integrated AMS, structural, palaeo- and rock-magnetic study of Eocene marine marls from the Jaca-Pamplona basin (Pyrenees, N Spain); new insights into the timing of magnetic fabric acquisition in weakly deformed mudrocks. In: Martín-Hernández, F., Lüneburg, C.M., Aubourg, C., Jackson, M. (Eds.), Magnetic Fabric: Methods and Applications.: Special Publication, 238. Geological Society, London, pp. 127–143.

Mattei, M., Funiciello, R., Kissel, C., 1995. Paleomagnetic and structural evidence for Neogene block rotations in the Central Apennines, Italy. Journal of Geophysical Research 100, 17863–17883.

Mattei, M., Sagnotti, L., Faccenna, C., Funiciello, R., 1997. Magnetic fabric of weakly deformed clayey sediments in the Italian peninsula: relationships with compressional and extensional tectonics. Tectonophysics 271, 107–122.

Parés, J.M., 2004. How deformed are weakly deformed mudrocks? Insights from magnetic anisotropy. In: Martín-Hernández, F., Lüneburg, C.M., Aubourg, C., Jackson, M. (Eds.), Magnetic Fabric: Methods and Applications.: Special Publication, 238. Geological Society, London, pp. 191–203.

Parés, J.M., van der Pluijm, B.A., 2002. Evaluating magnetic lineations (AMS) in deformed rocks. Tectonophysics 350, 283–298.

Parés, J.M., van der Pluijm, B.A., Dinarès-Turell, J., 1999. Evolution of magnetic fabrics during incipient deformation of mudrocks (Pyrenees, Northern Spain). Tectonophysics 307, 1–14.

Prokopenko, A.A., Khursevich, G.K., Bezrukova, E.V., Kuzmin, M.I., Boes, X., Williams, D.F., Fedenya, S.A., Kulagina, N.V., Letunova, P.P., Abzaeva, A.A., 2007. Paleoenvironmental proxy records of Lake Hovsgol, Mongolia, and a synthesis of Holocene climate change in the Lake Baikal watershed. Quaternary Research 68, 2–17.

Pueyo Anchuela, O., Pocoví Juan, A., Gil Imaz, A., 2010. Tectonic imprint in magnetic fabrics in foreland basins: a case study from the Ebro Bain, N Spain. Tectonophysics 492, 150–163.

Ramsay, J.G., Huber, M.I., 1983. The Techniques of Modern Structural Geology, Volume 1: Strain Analysis. Academic Press, London.

Reimer, P.J., Baillie, M.G.L., Bard, E., Bayliss, A., Beck, J.W., Blackwell, P.G., Ramsey, C.B., Buck, C.E., Burr, G.S., Edwards, R.L., Friedrich, M., Grootes, P.M., Guilderson, T.P., Hajdas, I., Heaton, T.J., Hogg, A.G., Hughen, K.A., Kaiser, K.F., Kromer, B., McCormac, F.G., Manning, S.W., Reimer, R.W., Richards, D.A., Southon, J.R., Talamo, S., Turney, C.S.M., van der Plicht, J., Weyhenmeye, C.E., 2009. IntCal09 and Marine09 radiocarbon age calibration curves, 0–50,000 years cal BP. Radiocarbon 51, 1111–1150.

Richter, C., van der Pluijm, B.A., Housen, B., 1993. The quantification of crystallographic preferred orientation using magnetic anisotropy. Journal of Structural Geology 15, 113–116.

Ricketts, R.D., Johnson, T.C., Brown, E.T., Rasmussen, K.A., Romanovsky, V.V., 2001. The Holocene paleolimnology of Lake Issyk-Kul, Kyrgyzstan: trace element and stable isotope composition of ostracodes. Palaeogeography, Palaeoclimatogy, Palaeoecology 176, 207–227.

Rull, V., Stansell, N.D., Montoya, E., Bezada, M., Abbott, M.B., 2010. Palynological signal of the Younger Dryas in the tropical Venezuelan Andes. Quaternary Science Reviews 29, 3045–3056.

Sagnotti, L., Speranza, F., Winkler, A., Mattei, M., Funiciello, R., 1998. Magnetic fabric of clay sediments from the external northern Apennines (Italy). Physics of the Earth and Planetary Interiors 105, 73–93.

Sagnotti, L., Winkler, A., Montone, P., Di Bella, L., Florindo, F., Mariucci, M.T., Marra, F., Alfonsi, L., Frepoli, A., 1999. Magnetic anisotropy of Plio-Pleistocene sediments from the Adriatic margin of the northern Apennines (Italy): implications for the time–space evolution of the stress field. Tectonophysics 311, 139–153.

Sintubin, M., 1994. Clay fabrics in relation to the burial history of shales. Sedimentology 41, 1161–1169.
Soto, R., Larrasoaña, J.C., Arlegui, L.E., Beamud, E., Oliva-Urcia, B., Simón, J.L., 2009. Reliability of magnetic fabric of weakly deformed mudrocks as a palaeostress indicator in compressive settings. Journal of Structural Geology 31, 512–522.
Tarling, D.H., Hrouda, F., 1993. The Magnetic Anisotropy of Rocks. Chapman & Hall, London.
Tauxe, L., 2005. Inclination flattening and the geocentric axial dipole hypothesis. Earth and Planetary Science Letters 233, 247–261.
Torizin, J., Jentzsch, G., Malischewsky, P., Kley, J., Abakanov, N., Kurskeev, A., 2009. Rating seismicity and reconstruction of the fault geometries in northern Tien Shan within the project "Seismic Hazard Assessment for Almaty". Journal of Geodynamics 48, 269–278.
Weaver, R., Roberts, A.P., Flecker, R., MacDonald, D.I.M., 2004. Tertiary geodynamics of Sakhalin (NW Pacific) from anisotropy of magnetic susceptibility fabrics and paleomagnetic data. Tectonophysics 379, 25–42.
Wu, Y., Li, S.J., Lucke, A., Wunnemann, B., Zhou, L.P., Reimer, P., Wang, S., 2010. Lacustrine radiocarbon reservoir ages in Co Ngoin and Zigê Tangco, central Tibetan Plateau. Quaternary International 212, 21–25.
Zijderveld, J.D.A., 1967. AC demagnetization of rocks: analysis of results. In: Collinson, D.W., Creer, K.M., Runcorn, S.K. (Eds.), Methods in Paleomagnetism. Elsevier, Amsterdam, pp. 254–286.